ACI STRUCTURAL JOURNAL TECHNICAL PAPER

Title no. 91-S43

Strength and Ductility of Concrete Columns Externally Reinforced with Fiber Composite Straps



by H. Saadatmanesh, M. R. Ehsani, and M. W. Li

Bridge failures in recent earthquakes such as the 1989 Loma Prieta earthquake have attracted the attention of the bridge engineering community to the large number of bridges with substandard seismic design details. Many concrete columns in bridges designed before the new seismic design provisions were adopted have low flexural ductility, low shear strength, and inadequate lap length for starter bars. These problems, compounded by flaws in the design of structural systems, have contributed to the catastrophic bridge failures in recent earthquakes. In this paper, a new technique for seismic strengthening of concrete columns is presented. The technique requires wrapping thin, flexible high-strength fiber composite straps around the column to improve the confinement and, thereby, its ductility and strength. Analytical models are presented that quantify the gain in strength and ductility of concrete columns externally confined by means of high-strength fiber composite straps. A parametric study is conducted to examine the effects of various design parameters such as concrete compressive strength, thickness and spacing of straps, and type of strap. The results indicate that the strength and ductility of concrete columns can be significantly increased by wrapping high-strength fiber composite straps around the columns.

Keywords: columns (supports); concretes; **ductility**; **fibers**; strapping; **strength**.

The 1971 San Fernando earthquake, the 1987 Whittier earthquake, and the 1989 Loma Prieta earthquake inflicted substantial damage on a number of older bridge structures. One of the major causes of the failure of those bridges was the substandard detailing of those structural components designed before the current seismic design provisions had been adopted. The inadequate detailing of these structures has resulted in many bridges having columns with low flexural strength, low shear strength, and low flexural ductility. The inadequate starter bar lap lengths and insufficient lateral ties in these columns are the major contributors to their insufficiency in resisting earthquake forces.

The work of many researchers has indicated that increasing the confinement in the potential plastic hinge regions of the column will increase the compressive strength of the core concrete and ultimate concrete compression strain and ductility. Therefore, strengthening techniques typically involve methods for increasing the confining forces either in the potential plastic hinge regions or over the entire column.[1]

In this paper, a new technique for seismic strengthening of concrete columns is presented. Columns in existing structures are externally reinforced by means of high-strength fiber composite straps. The reinforcement is performed by wrapping straps of desired width and thickness around the columns. The straps can be wrapped in a continuous spiral and/or in discontinuous rings. The straps are constructed from high-strength fibers woven to form a flexible fabric-like material. The fabrics can be made very thin, resulting in flexibility sufficient for them to be wrapped around circular as well as rectangular columns. For improved structural performance as well as protection against environmental factors, the straps can be impregnated with resin either before or after the wrapping operation. The ends of the straps can be mechanically coupled or they can be epoxy-bonded to the column. Fig. 1 shows typical concrete columns externally confined with fiber composite straps. This method is a spinoff of another study performed by the authors, where concrete girders were strengthened by means of composite laminates bonded to the tension face of the girders.[2-4] In some of the girders tested, the ultimate strength was increased by a factor of 4. The salient benefits of strengthening concrete columns with fiber composite straps are summarized in the following:

Increased ductility—As a result of the confinement provided by the straps, the concrete will fail at a larger strain than if unconfined. Depending on the degree of confinement, significant increases in ductility can be achieved.

Increased strength—The lateral pressure exerted by the straps will increase the compressive strength of the concrete in both the core and shell regions, resulting in higher load-carrying capacity. The lateral confinement provided by the

ACI Structural Journal, V. 91, No. 4 July-August 1994.
Received June 25, 1993, and reviewed under Institute publication policies. Pertinent discussion will be published in the May-June 1995 *ACI Structural Journal* if received by Jan. 1, 1995.

Hamid Saadatmanesh *is Associate Professor of Civil Engineering and Engineering Mechanics at the University of Arizona, Tucson. His primary area of research is in applications of advanced composite materials for strengthening and rehabilitation of structures. He is Secretary of ACI Committee 440, Fiber Reinforced Plastic Reinforcement.*

Mohammad R. Ehsani *is Associate Professor of Civil Engineering and Engineering Mechanics at the University of Arizona. He is a member of ACI Committee 408, Bond and Development of Reinforcement. He is also Secretary of ACI Committee 352, Joints and Connections in Monolithic Structures. Dr. Ehsani is a registered professional engineer in Arizona and California.*

Mu-Wen Li *is a structural designer at SUNDT Construction Company, Taipei, Taiwan. He was formerly a graduate student in the Department of Civil Engineering and Engineering Mechanics, the University of Arizona.*

straps will also provide additional support against buckling of the longitudinal bars.

Circular and square sections—The flexibility of the straps allows wrapping around circular as well as rectangular columns.

Low maintenance—Because of their resistance to electrochemical deterioration, fiber composites do not corrode and are not affected by salt spray, and other aggressive environmental factors. Ultraviolet light, however, can adversely affect some fiber composites. This problem can be eliminated by providing a protective coating for the straps during or after the manufacturing process.

Low weight—The low density of composites (typically one-fifth that of steel) significantly simplifies the construction procedure and reduces cost.

Temporary versus permanent—The proposed method will cause no disturbance to the integrity of the existing structure; i.e., no anchor bolts, dowels, etc., will be required when the ends of the straps are mechanically coupled. As a result, this method can be used as a permanent or temporary solution. For example, if, at a later time, more effective alternatives are developed, the straps can be easily removed.

Esthetics—The straps are very thin, i.e., less than 100 mils thick; therefore, they will not alter the appearance of the structure.

In this paper, analytical models are presented for the analysis of concrete columns under monotonic loading and externally confined with fiber composite straps. A parametric study is also conducted to examine the effectiveness of this technique for increasing the strength and ductility of concrete columns.

RESEARCH SIGNIFICANCE

The devastation caused by the 1989 Loma Prieta earthquake clearly attests to the need for effective seismic strengthening techniques to prevent such failure in the future. The method presented in this paper will provide an economical and effective alternative for increasing the strength and ductility of columns with inadequate transverse reinforcement. Furthermore, the utilization of such advanced modern materials as fiber composites will provide a new outlook on design of concrete structures. Fiber composites generally have higher strength-to-weight ratios than conventional materials and are unaffected by electrochemical deterioration.

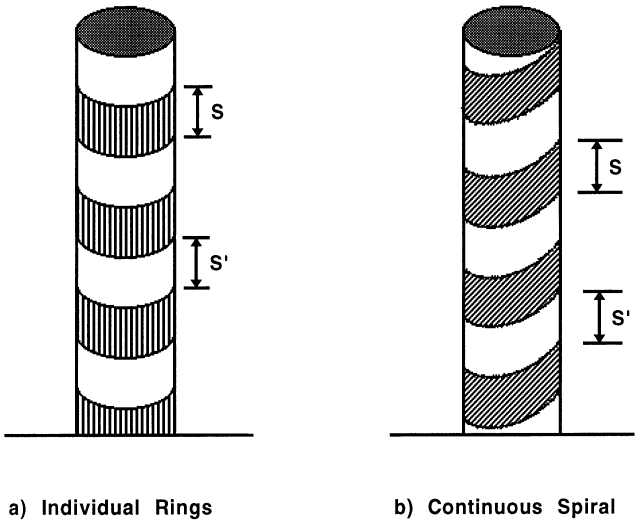

Fig. 1—Column wrapped with composite straps

PREVIOUS WORK

External confinement with steel (steel jacketing) has been used to improve the shear strength and ductility of columns.

To investigate the performance of the columns retrofitted with steel jacketing, six large-scale column models were tested at the University of California at San Diego.[1] The columns were 0.4-scale models of a prototype 1524-mm- (60-in.)-diameter bridge column. They were 610 mm (24 in.) in diameter and 3657 mm (12 ft) in height. The test columns were constructed with a footing to allow foundation influence or interaction to be monitored. The tests included models with the pre-1971 reinforcing details without retrofitting, columns retrofitted with steel jackets, and a post-damage retrofitted column to determine whether a damaged column can be salvaged after an earthquake. The longitudinal steel reinforcement ratio was 2.53 percent. Transverse reinforcement consisted of circular hoops (No. 2 Grade 40 plain bars) placed at 127 mm (5 in.) on centers uniformly along the longitudinal line of the column. The confining steel reinforcement ratio was 0.18 percent. The hoops were spliced with a lap length of 305 mm (12 in.) in the cover concrete. Steel jackets for the columns were fabricated from 4.76-mm- ($^3/_{16}$-in.)-thick A36 hot-rolled steel. A 6.3-mm ($^1/_4$-in.) gap was provided between the column and jacket. The gap was pressure-injected with water/cement grout.

From the test results, it was concluded that a lap length of 20 times the longitudinal bar diameter was insufficient to develop yield stress of the longitudinal bars; columns without retrofitting degraded rapidly due to bond failure. The confinement provided by a fully grouted steel jacket could completely contain the cover concrete to eliminate bond failure. Also, because there was only a 10 to 20 percent increase in lateral stiffness due to additional confinement from the steel jacket, a ductile mode of flexural failure with good energy dissipation could be achieved. The steel jacket enabled a displacement ductility factor of greater than 6 to be achieved.

Katsumata, Kobatake, and Takeda,[5] tested 10 one-quarter-scale column specimens with square cross sections of 200 x 200 mm (7.87 x 7.87 in.). The columns were strengthened with carbon fiber wraps before testing. They were tested un-

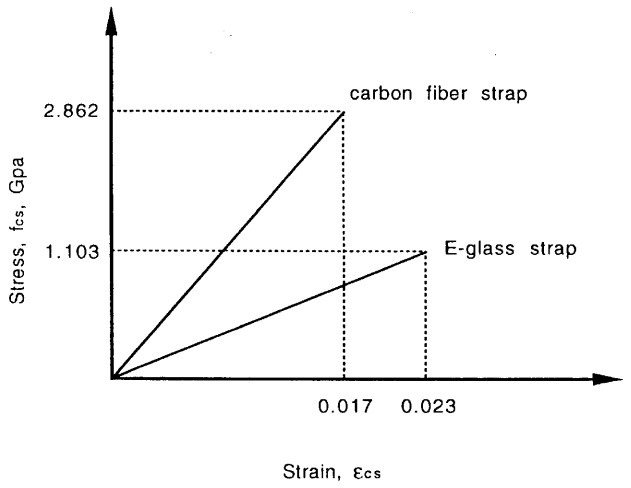

Fig. 2—Stress-strain curves of composite straps

der cyclic lateral loads and a constant axial load. It was concluded that winding of carbon fiber has ample effect on increasing seismic capacity. In particular, the following factors were determined: 1) ultimate displacement and energy dissipation was increased approximately linearly in accordance with carbon fiber quantity; 2) the earthquake-resistant capacity of a carbon fiber-strengthened column can be correlated roughly with an ordinary reinforced concrete column with only hoop reinforcement; and 3) carbon fiber quantity and steel hoop reinforcement quantity could be mutually convertible by effective strength ratio.

Recently, a test conducted by the University of California at San Diego involved a new type of fiberglass-epoxy composite material,[6] made of high modular and regular glass fibers, and wrapped like a blanket in layers around a 3657-mm (12-ft)-high test column. The column size and reinforcement were representative of many of the columns built on the California State Highway system prior to 1971.

Two tests of columns retrofitted with this material were conducted. For the first test, the column was wrapped with eight layers of the material [2.44-mm (0.096-in.) nominal thickness] and pressure-grouted to 1.76 MPa (250 psi) by pumping epoxy between the concrete and the wrap. The second involved wrapping a test column with four layers of the material pressurized to 1.06 MPa (150 psi). A vertical load of 1816 kN (400 kips) was applied to the column in each test.

Application of lateral load and displacement consisted of a series of cycles of imposed inelastic displacements from ± 2.54 to 254 mm (±1 to 10 in.). The columns were pushed and pulled far beyond their yield point, which probably exceeds the displacement expected in maximum credible earthquakes. Even though the concrete crushed and some steel reinforcing bars ruptured in tension during the test, the fiber wrap remained intact.

FIBER COMPOSITES

The use of composites for a variety of industrial applications has been rapidly increasing in recent years. The main reasons for using these types of materials are their superior strength-to-weight ratio, and durability in corrosive environments, as compared with conventional materials. In addition to the superior strength properties, many composites have shown much better fatigue performance than structural metals.

Fiber composites have been used extensively in the aircraft and aerospace industries. The first recorded application of glass-fiber composites in the aircraft industry dates as far back as 1944.[7] Since then, a variety of composites have been used in such industries as ship building, chemical processing, medical, automotive, etc.

Composites are made up of short fibers or filaments of glass, carbon, etc., bonded together with a resin matrix. The fibers provide the composites with their unique structural properties. The matrix serves only as a bonding agent.

Two types of resin-impregnated unidirectional composite straps will be used in this study. The following is a brief description of the mechanical properties of the two types of straps: namely, E-glass and carbon fiber straps.

E-glass strap

Glass fiber reinforced composites are among the oldest and least expensive of all composites. Fiberglass is widely used in automotive, marine, sporting goods, and aerospace applications. E-glass is the most common type of glass fiber used in resin matrix composite structures. The individual fibers of E-glass have tensile strength in excess of 3.45 GPa (500 ksi).[8] These fibers range from 3 to 5 microns in diameter. The principal advantages of E-glass are low cost, high tensile and impact strengths, and high chemical resistance. The disadvantages of E-glass, compared to other structural fibers, are lower modulus, lower fatigue resistance, and higher fiber self-abrasion characteristics. The modulus of elasticity of E-glass in the fiber form is 72.4 GPa (10.5×10^3 ksi). The density and coefficient of thermal expansion of E-glass are 2.5 g/cm^3 (0.092 lb/in.^{3}) and 5×10^{-6} cm/cm/C (2.8×10^{-6} in./in./F), respectively.

In general, fiber composites behave linearly elastic to failure. The tensile strength and modulus of elasticity of composites, i.e., resin plus fiber, based on gross cross-sectional area, are smaller than the strength and modulus of the constituent fiber itself. The manufacturer provided the following information on unidirectional E-glass composite (resin plus fiber) tapes that could be used to wrap concrete columns:[9] tensile strength = 1103 MPa (160 ksi) and modulus of elasticity = 48.2 GPa (7×10^3 ksi). Fig. 2 shows the stress-strain behavior of E-glass tapes used in this study.

Carbon fiber strap

Carbon fiber is another suitable material for retrofitting of concrete columns. It is convenient to classify carbon fiber into four different performance groups, based on tensile modulus, strength, or precursor type. They are standard modulus, intermediate modulus, high modulus, and pitch fibers.[10]

The following is a brief description of the properties of those four groups.

Standard modulus—Standard modulus fibers have tensile strengths in the 2.4 to 3.1 GPa (350 to 450 ksi) range. Advances in fiber technology have brought about high-strength fibers, those with tensile strength greater that 3.445 GPa

(500 ksi). Ultimate strain-to-failure ranges from 1.4 to 1.8 percent.

Intermediate modulus—Intermediate modulus fiber has typical modulus values ranging from 274 to 315 GPa (40 to 46×10^3 ksi). Ultimate strain-to-failure ranges from 1.5 to 2.0 percent.

High modulus—High modulus fiber's typical modulus values extend over 345 GPa (50×10^3 ksi). Ultimate strain-to-failure is low, ranging from 0.3 to 0.5 percent.

Pitch fiber—Pitch fibers generally fall into categories of high modulus, 345 to 485 GPa (50 to 70×10^3 ksi), or ultra-high modulus, 485 to 825 GPa (70 to 120×10^3 ksi). Ultimate strain-to-failure ranges from 0.3 to 0.5 percent.

To obtain higher confinement pressure and ductility in concrete columns, unidirectional tapes of intermediate modulus carbon fiber will also be used in this study. The following information is obtained from the data provided by the manufacturer for intermediate carbon tapes:[10] tensile strength = 2.862 GPa (415 ksi); modulus of elasticity = 172 GPa (25×10^3 ksi). Fig. 2 shows the stress-strain curve of the carbon tape used in the study.

ANALYTICAL MODELS

Stress-strain models for confined concrete, developed by Mander, Priestley, and Park[11] and based on an equation proposed by Popovics,[12] were used in the analysis of circular and rectangular columns confined with composite straps. The models were included in a computer program developed to predict the ultimate moment and curvature at failure of the columns from pure compression to pure bending. The following assumptions were made in the analysis: linear strain distribution through full depth of the cross section; small deformations; no creep and shrinkage deformations; no shear deformation; no tensile strength for concrete; complete composite action between confining composite materials and concrete column, i.e., no slip; no confinement contribution from original stirrups; and uniform confinement at corners and along sides of rectangular sections.

Stress-strain relationships of materials

Concrete for circular columns—The stress-strain models of confined and unconfined concrete in circular sections in compression proposed by Mander et al.,[11,13] and based on the work of several other researchers[12,14-16] will be summarized here and adopted for the analysis of concrete columns externally reinforced with fiber composite straps. The stress-strain model shown in Fig. 3 is based on an equation proposed by Popovics.[12] For a slow strain rate and monotonic loading, the longitudinal compressive concrete stress f_c is defined by the following equation

$$f_c = \frac{f_{cc}' x r}{r - 1 + x^r} \tag{1}$$

where

$$x = \frac{\varepsilon_c}{\varepsilon_{c\,c}} \tag{2}$$

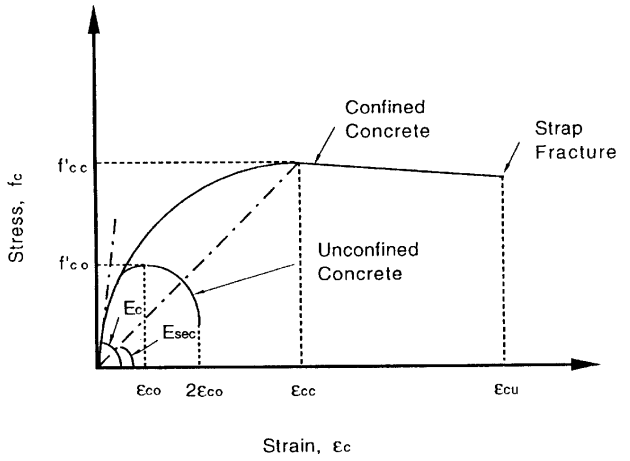

Fig. 3—Stress-strain model proposed for unconfined and confined concrete

$$\varepsilon_{cc} = \varepsilon_{co}\left[1 + 5\left[\frac{f_{cc}'}{f_{co}'} - 1\right]\right] \tag{3}$$

$$r = \frac{E_c}{E_c - E_{\text{sec}}} \tag{4}$$

$$E_{\text{sec}} = \frac{f_{cc}'}{\varepsilon_{cc}} \tag{5}$$

$$f_{cc}' = f_{co}'\left[-1.254 + 2.254\sqrt{1 + \frac{7.94 f_l'}{f_{co}'}} - 2\frac{f_l'}{f_{co}'}\right] \tag{6}$$

where f_{cc}' = compressive strength of confined concrete; f_{co}' = unconfined concrete strength; ε_c = longitudinal compressive strain of concrete; ε_{cc} = strain at maximum concrete stress f_{cc}' of confined concrete; ε_{co} = 0.002, strain at maximum concrete stress f_{co}' of unconfined concrete; E_c = tangent modulus of elasticity of concrete E_{sec} = secant modulus of confined concrete at peak stress; and f_l' = effective lateral confining pressure from transverse reinforcement, assumed to be uniformly distributed over the surface of the concrete core.

Mander et al.[11] proposed an effective lateral confining pressure by transverse reinforcements on the circular concrete section. This effective pressure is defined as

$$f_l' = f_l k_e \tag{7}$$

where

$$k_e = \frac{A_e}{A_{cc}} \tag{8}$$

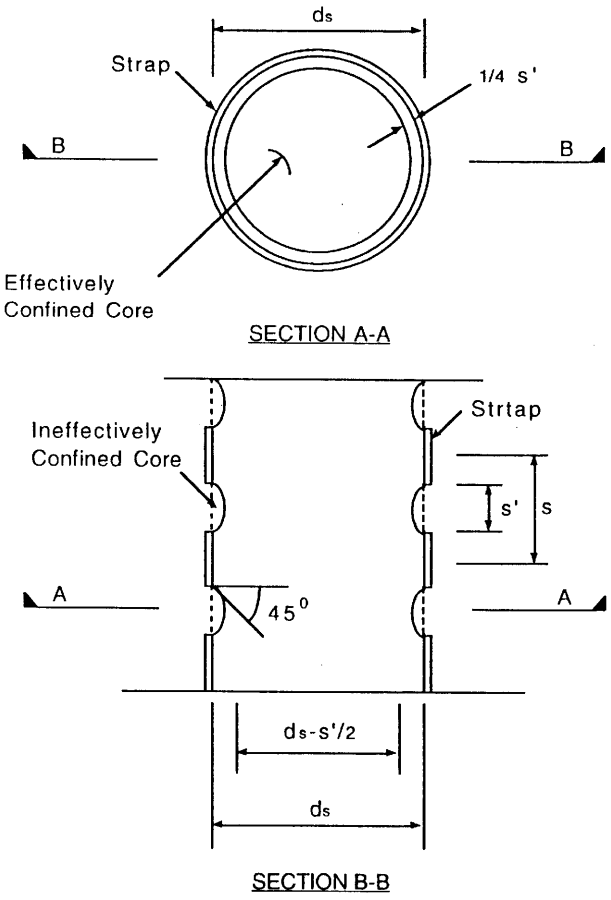

Fig. 4—Confinement of circular column

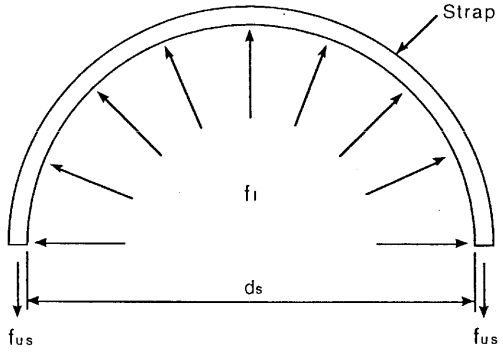

Fig. 5—Confining action of composite strap

where f_l = lateral pressure from transverse reinforcement; k_e = confinement effectiveness coefficient; A_e = area of effectively confined concrete core; and A_{cc} = effective area of concrete enclosed by composite strap given by

$$A_{cc} = A_c(1 - \rho_{cc}) \tag{9}$$

where ρ_{cc} = ratio of area of longitudinal reinforcement to gross area of concrete; and A_c = area of concrete enclosed by composite strap.

A technique proposed by Sheikh and Uzumeri[17] is used to determine the area of effectively confined concrete between the composite straps. As shown in Fig. 4, it is assumed that an arching action occurs between straps in the form of a second-degree parabola with an initial tangent slope of 45 deg. The concrete within this parabola is assumed to be ineffective. The smallest area of confined concrete occurs midway between the straps and is calculated from

$$A_e = \frac{\pi}{4}\left(d_s - \frac{s'}{2}\right)^2 = \frac{\pi}{4}d_s^2\left(1 - \frac{s'}{2d_s}\right)^2 \tag{10}$$

where s' = clear vertical spacing between straps; and d_s = diameter of column.

From Eq. (8) through (10), the confinement effectiveness coefficient for circular sections can be calculated as

$$k_e = \frac{\left(1 - \frac{s'}{2d_s}\right)^2}{1 - \rho_{cc}} \tag{11}$$

The confining pressure induced on the concrete core by the composite strap is calculated by considering the free body of the circular cross section confined by the strap, as shown in Fig. 5. The outward expansion of the core concrete is prevented by the action of the strap placed in circumferential tension. From equilibrium of forces, the confining stress f_l can be calculated as

$$f_l = \frac{2f_{us}A_{st}}{d_s s} \tag{12}$$

where f_{us} = ultimate strength of composite strap; A_{st} = cross-sectional area of strap; and s = width of strap. The volumetric ratio of confining strap to concrete core ρ_s is given by

$$\rho_s = \frac{A_{st}\pi d_s}{\frac{\pi}{4}d_s^2 s} = \frac{4A_{st}}{d_s s} \tag{13}$$

Solving Eq. (13) for the ratio $A_{st}/d_s s$ and substituting into Eq. (12) results in

$$f_1 = \frac{1}{2}\rho_s f_{us} \tag{14}$$

The lateral pressure f_l calculated from Eq. (14) can be substituted into Eq. (7) to determine the effective lateral confining pressure f_l'.

To calculate the longitudinal compressive strain of confined concrete at failure ε_{cu}, the approach proposed by Mander et al.[11] and Scott, Park, and Priestley,[16] based on an energy balance concept, is used. In this approach, the additional ductility available when concrete is confined is considered to be due to energy stored in the confining composite straps.

In Fig. 3, for unconfined and confined concrete, the area under each stress-strain curve represents the total strain en-

ergy per unit volume of concrete at failure. The difference between these two areas is provided for by the confining effect of the composite strap, as given by the following equation

$$U_{st} = U_{cc} + U_{sl} - U_{co} \quad (15)$$

where U_{co} = ultimate strain energy per unit volume of unconfined concrete given by

$$U_{co} = A_c \int_0^{2\varepsilon_{co}} f_{uc} d\varepsilon_c \quad (16)$$

U_{sl} = energy required to maintain yield in longitudinal steel in compression given by

$$U_{sl} = \rho_{cc} A_c \int_0^{\varepsilon_{cu}} f_{sl} d\varepsilon_{sl} \quad (17)$$

U_{cc} = ultimate strain energy per unit volume of confined concrete

$$U_{cc} = A_c \int_0^{\varepsilon_{cu}} f_c d\varepsilon_c \quad (18)$$

U_{st} = ultimate strain energy per unit volume of composite strap given by

$$U_{st} = \rho_s A_c \int_0^{\varepsilon_{us}} f_{st} d\varepsilon_{st} \quad (19)$$

where ε_{us} = ultimate strain of composite strap; ε_{cu} = strain in concrete at the point when composite strap ruptures; f_{st} and ε_{st} = stress and strain in composite strap; and f_{sl} = stress in longitudinal reinforcement.

Substituting Eq. (16) through (19) into Eq. (15) and solving for ε_{cu}, the ultimate compression strain of concrete at the point of fracture of the confining composite strap can be calculated, resulting in complete determination of the stress-strain curve of the confined concrete throughout the entire range of loading, up to the fracture of composite strap and consequent failure of the column.

Concrete for rectangular sections—To extend the stress-strain relationship of concrete described in the previous section to that for rectangular cross sections, it will be necessary to modify the effective lateral confining pressure f_l'. Assuming again that arching action occurs in the form of a second-degree parabola, as was shown in Fig. 4 for circular columns, the area of effectively confined concrete core midway between the levels of straps can be calculated from

$$A_e = \left(h - \frac{s'}{2}\right)\left(b - \frac{s'}{2}\right) = hb\left(1 - \frac{s'}{2h}\right)\left(1 - \frac{s'}{2b}\right) \quad (20)$$

where b and h = cross-sectional dimensions.

Substituting Eq. (9) and (20) into Eq. (8) results in the confinement effectiveness coefficient for rectangular sections given by the following

$$k_e = \frac{\left(1 - \frac{s'}{2h}\right)\left(1 - \frac{s'}{2b}\right)}{1 - \rho_{c\,c}} \quad (21)$$

The rest of the procedure for determining the effective lateral confining pressure f_l' is similar to that of the circular columns and will not be repeated here.

The stress-strain behavior of steel is idealized as elastic-perfectly plastic.

Composite straps—Composite straps behave linearly elastic to failure. Fig. 2 shows the stress-strain relationships for E-glass and carbon fiber composite straps used in this study.

The strain compatibility method was used to calculate the strains across the depth of the cross section. Given the value of concrete strain in the extreme compression fiber, the steel strain in reinforcing bars can be described in terms of the concrete strain and depth of the neutral axis c. The depth of the neutral axis c is then obtained by considering the equilibrium of forces across the cross section. Knowing the location of the neutral axis, the strains in the concrete and steel reinforcing bars can be calculated from similar triangles in the strain diagram. The stresses in concrete and steel reinforcing bars may then be found from the stress-strain curves of concrete and steel. The forces in the concrete and steel reinforcing bars are calculated by multiplying their stresses by their corresponding areas. Knowing the forces in the concrete and steel reinforcing bars, the axial load is obtained from equilibrium of forces. The moment is calculated by multiplying the forces in the concrete and steel reinforcing bars by distances between their corresponding locations and the plastic centroid of the column. The curvature is obtained by dividing the strain in the extreme compression fiber of concrete by the depth of the neutral axis. A computer program was developed to carry out the numerical calculations.

PARAMETRIC STUDY

A parametric study was conducted on the behavior of circular and rectangular columns strengthened with composite straps.

The following are the major variable parameters used in the study.

Three values of unconfined concrete compressive strengths were used: f_{co}' = 20.67, 27.56, and 34.45 MPa (3000, 4000, and 5000 psi).

Three strap thicknesses were used in this study: t = 5, 10, and 15 mm (0.197, 0.394, and 0.591 in.).

Three values of clear spacings were used: s´ = 0.0, 152.4, and 305 mm (0.0, 6.0, and 12.0 in.).

Two types of straps were used in the study: E-glass and carbon fiber. The stress-strain relationship to failure for these straps is shown in Fig. 2.

Axial load-moment-curvature diagrams as well as plots of ductility factor φ_u/φ_y versus axial load ratio P/P_o, strap thickness t, and clear spacing between straps s'; and plots of moment ratio, M_u/M_y versus strap thickness t were generat-

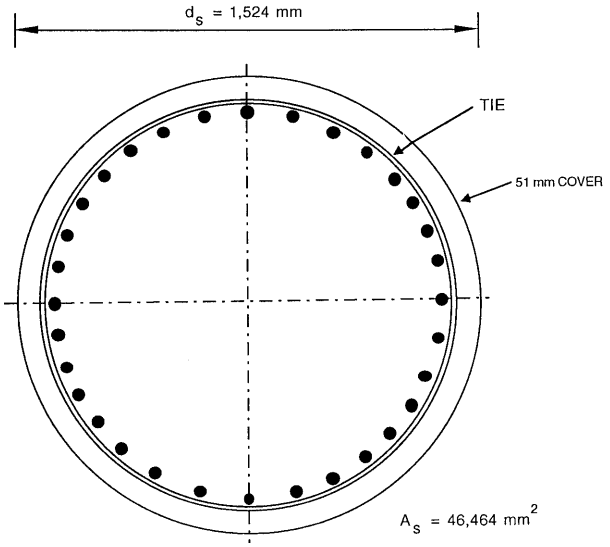

Fig. 6—Cross section and reinforcement details of circular column used in parametric study

ed using different combinations of variable parameters discussed previously. The variables shown on the plots are: P = axial load; P_0 = ultimate axial load of unconfined column; φ_y = curvature at first yield of tension steel; φ_u = curvature at failure of confined column; M_y = moment at first yield of tension steel of unconfined column; M_u = moment at failure of confined column; t = thickness of composite strap; and s' = clear spacing between straps. In these plots, each column is identified with an acronym, where the first symbol stands for the cross section type, i.e., C = circular column and R = rectangular column; the second symbol stands for compressive strength of concrete, i.e., 3 indicates 20.67 MPa (3000 psi), 4 indicates 27.56 MPa (4000 psi), and 5 indicates 34.45 MPa (5000 psi); the third symbol stands for thickness of strap, i.e., T5 indicates t = 5 mm (0.197), T10 indicates t = 10 mm (0.394 in.), and T15 indicates t = 15 mm (0.591 in.); and the fourth symbol stands for clear spacing between straps, i.e., S´0 indicates s' = 0.0 mm (0.0 in.), S´18 indicates s' = 152.4 mm (6 in.), and S´12 indicates s' = 305 mm (12.0 in.).

Circular columns

A prototype bridge column was used in the parametric study.[1] Fig. 6 shows the reinforcement details of the column. A 152-mm (6-in.)-wide strap was used for retrofitting. Grade 60 steel reinforcing bar was used for the longitudinal reinforcement.

Fig. 7(a) through (c) shows the plots of the interaction diagrams and curvature ductility for the column for three different concrete compressive strengths. The interaction diagrams and curvature ductility curves for the same section without strap are shown with dotted lines in each graph. From the interaction diagrams in the figures, it can be seen that the ultimate axial load is increased by 103, 92, and 82 percent for the column strengthened with E-glass strap, and 171, 162, and 151 percent for the column strengthened with carbon fiber strap, respectively, compared with the strength of an unretrofitted column. The maximum moment capacity is increased by 53, 48, and 45 percent for the column strengthened with E-glass strap, and 87, 83, and 79 percent for the column strengthened with carbon fiber strap, respectively, compared with the moment capacity of an unconfined column. The increase in maximum moment capacity is less than that in the ultimate axial load. This is not a shortcoming of this strengthening technique, since the majority of columns requiring strengthening lack adequate ductility, not flexural capacity. In fact, it is desirable to increase the ductility without increasing the moment capacity to prevent a brittle failure. From the plots of curvature ductility, it can be seen that the ductility factor φ_u/φ_y increases significantly as a result of confinement provided by the composite strap. However, this value does not change appreciably for the three different concrete compressive strengths.

Fig. 8(a) through (c) shows the plots of the interaction diagrams and curvature ductility for the three different values of clear spacing between straps. A 152-mm (6-in.)-wide strap was used for these figures. As can be seen from the figures, the ultimate axial load is increased by 82, 44, and 29 percent for strengthening with E-glass strap, and 151, 92, and 63 percent for strengthening with carbon fiber strap, respectively, compared with the values prior to strengthening. The maximum moment capacity is increased by 45, 25, and 17 percent for strengthening with E-glass strap, and 79, 47, and 33 percent for strengthening with carbon fiber strap, respectively. As before, the increase in the maximum moment capacity is less than that in the ultimate axial load. From the plots of curvature ductility, it can be seen that larger strap spacings decrease the ductility factor significantly. In Fig. 8(c), when a clear spacing of s' = 304.8 mm (12.0 in.) is used, the ductility factor of the section strengthened with E-glass is almost the same as that before strengthening.

Fig. 9(a) through 9(c) shows the plots of interaction diagrams and curvature ductility for the section for different thicknesses of the E-glass and carbon fiber straps. The figures show that the ultimate axial load is increased by 82, 130, and 163 percent for the section strengthened with E-glass strap, and 151, 208, and 235 percent for the same section strengthened with carbon fiber strap, respectively, compared to the ultimate axial load before strengthening. The maximum moment capacity is increased by 45, 75, and 98 percent for E-glass strap, and 79, 120, and 148 percent for the carbon fiber strap, respectively. From the plots of the interaction diagrams and curvature ductility, it can be seen that the ductility factor increases significantly as the thickness of strap increases.

Fig. 10 shows the relationship between ductility factor φ_u/φ_y and strap thickness t for E-glass and carbon fiber straps for a typical retrofitted column. As can be seen from these graphs, the ductility factor is increased almost linearly with increasing thickness of the strap. However, the rate of increase of ductility factor decreases with an increase in the clear spacing between straps. A similar trend was also observed for other columns with different f_{co}' and P/P_o; however, the ductility ratio φ_u/φ_y decreases for higher concrete compressive strengths.

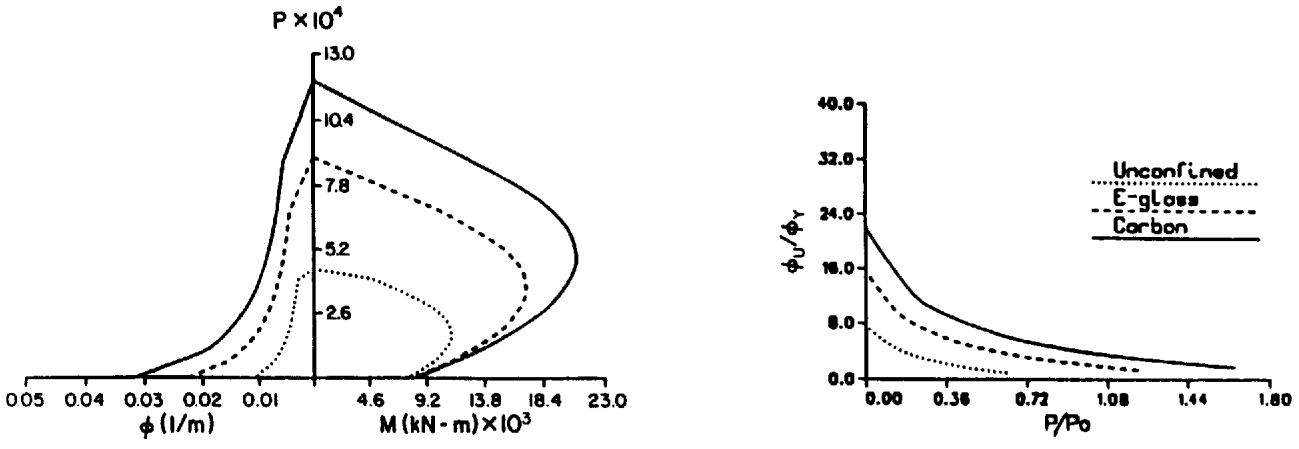

a) Column C3T5S´O

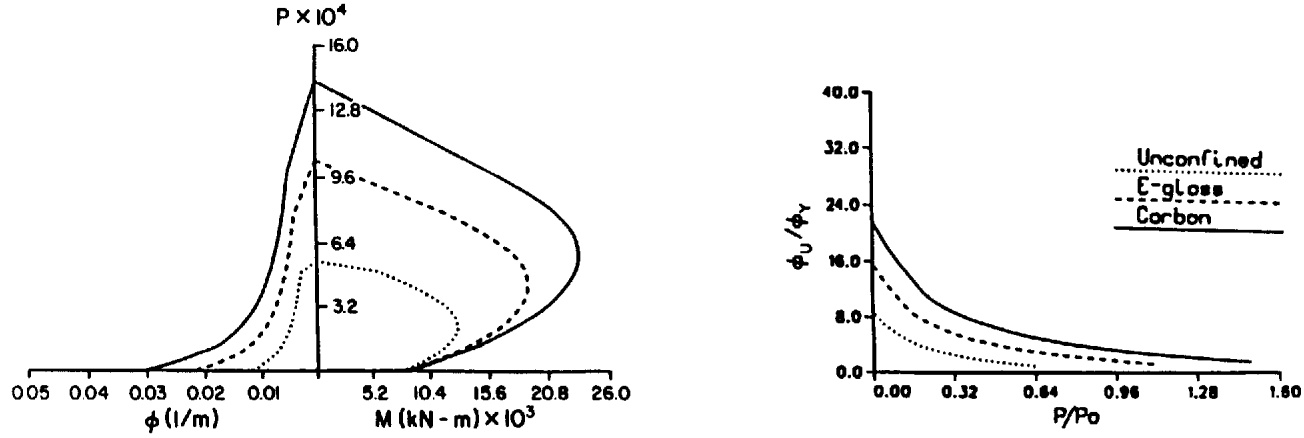

b) Column C4T5S´O

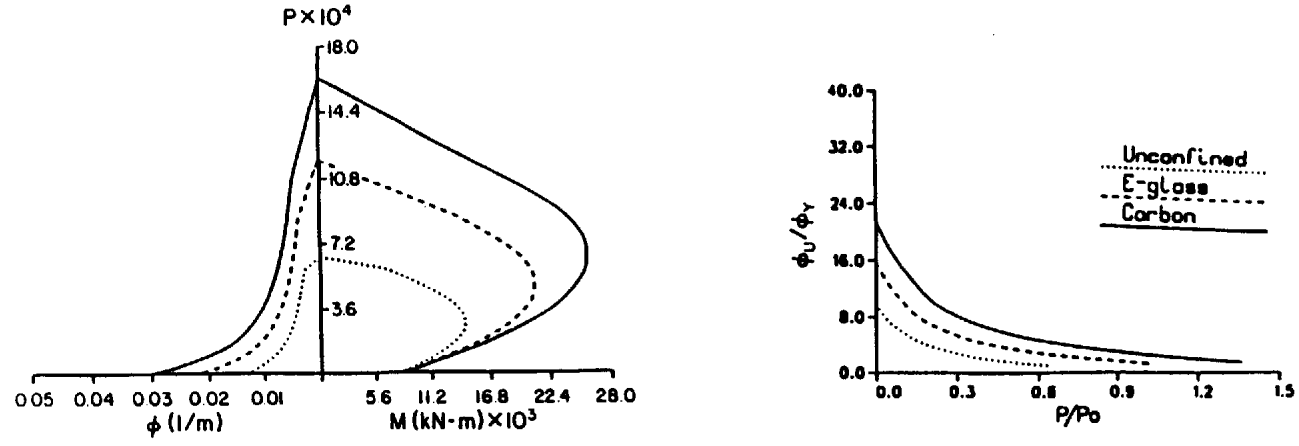

c) Column C5T5S´O

Fig. 7—Interaction diagram and ductility factor of circular column for three different concrete compressive strengths

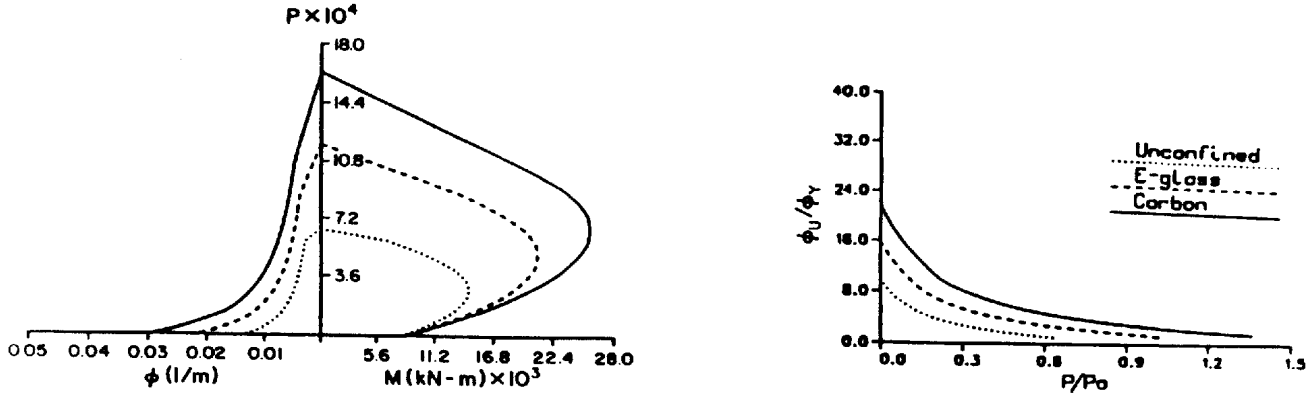

a) Column C5T5S´O

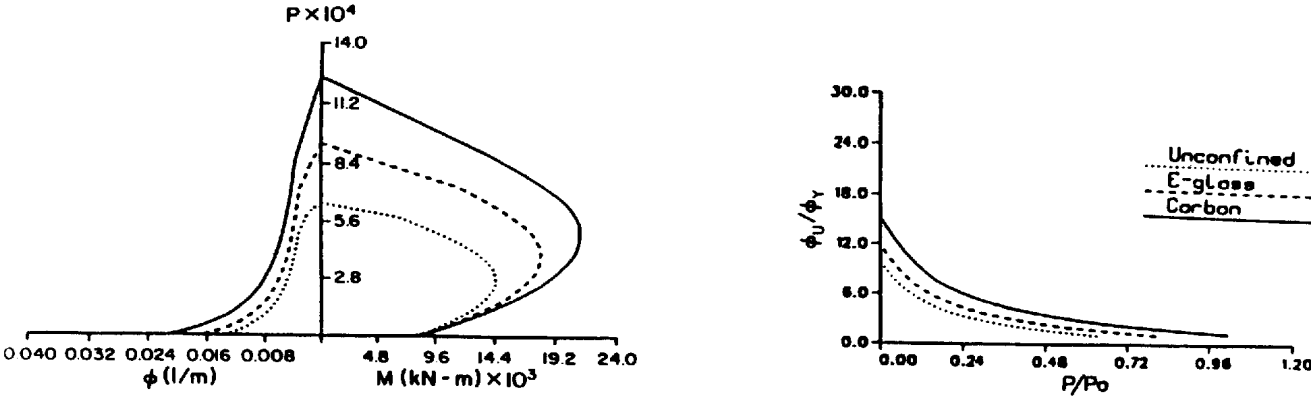

b) Column C5T5S´6

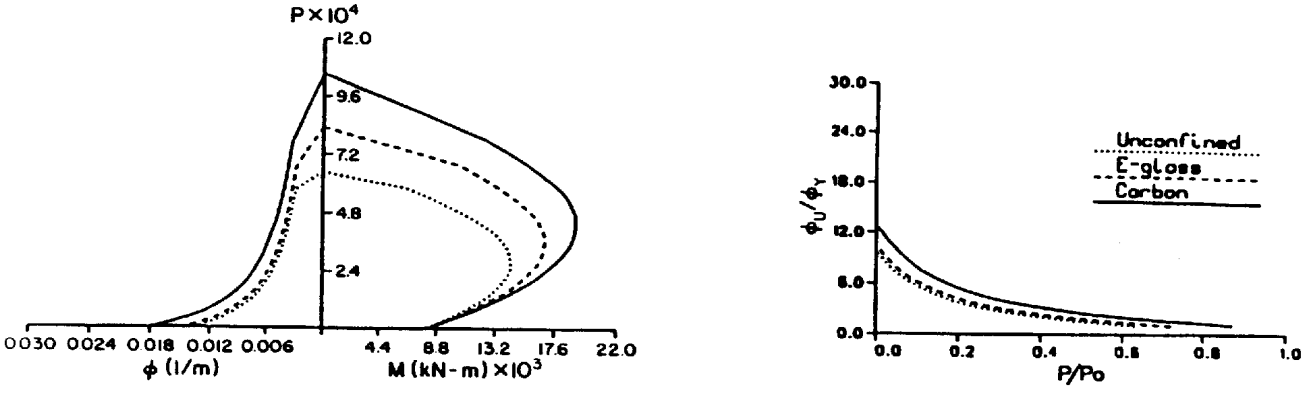

c) Column C5T5S´12

Fig. 8—Interaction diagram and ductility factor of circular column for three different spacings between straps

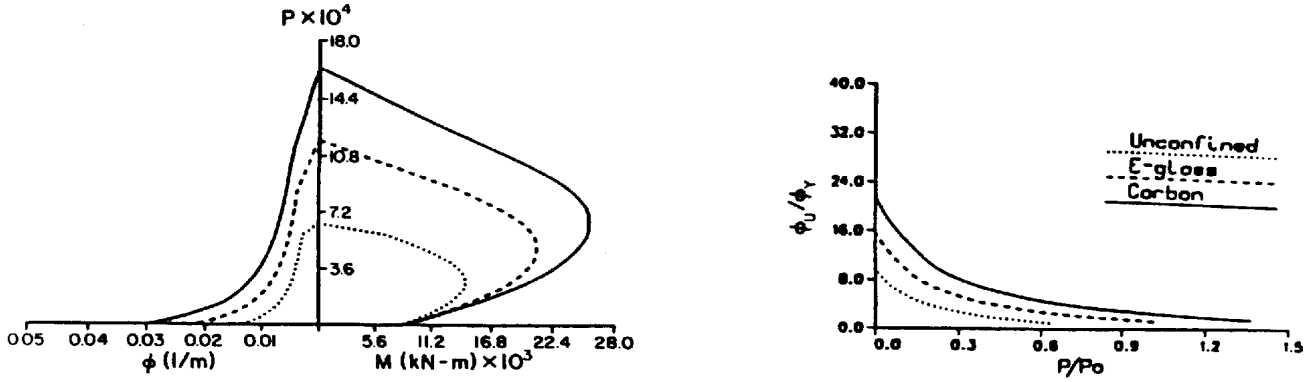

a) Column C5T5S´0

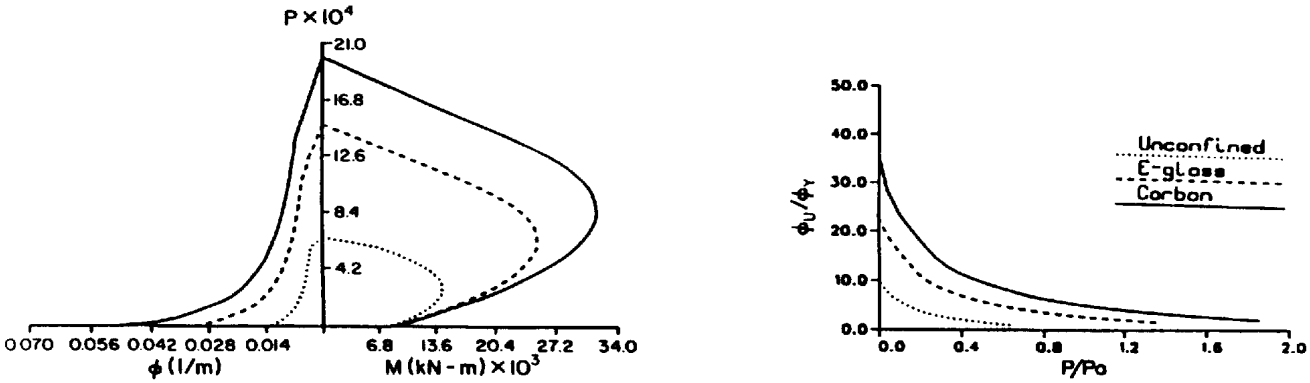

b) Column C5T10S´O

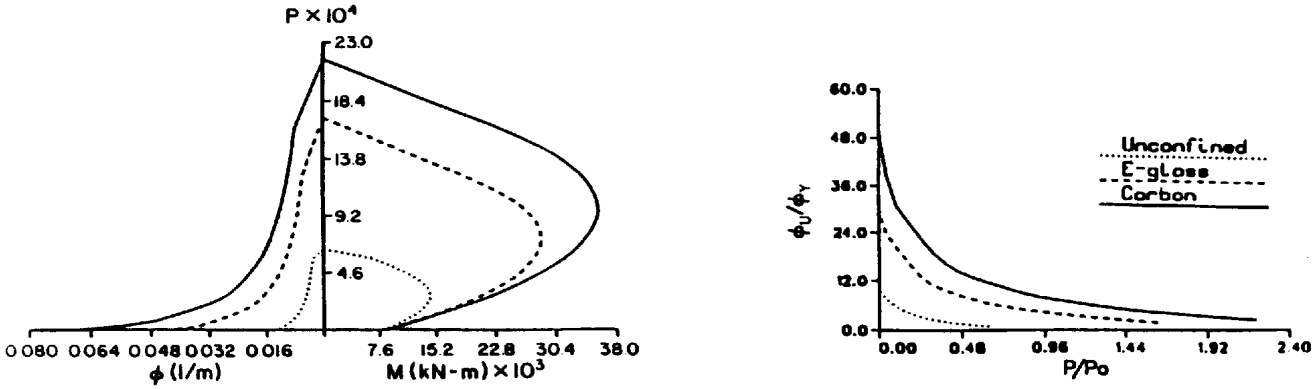

c) Column C5T15S´O

Fig. 9—Interaction diagram and ductility factor of circular column for three different strap thicknesses

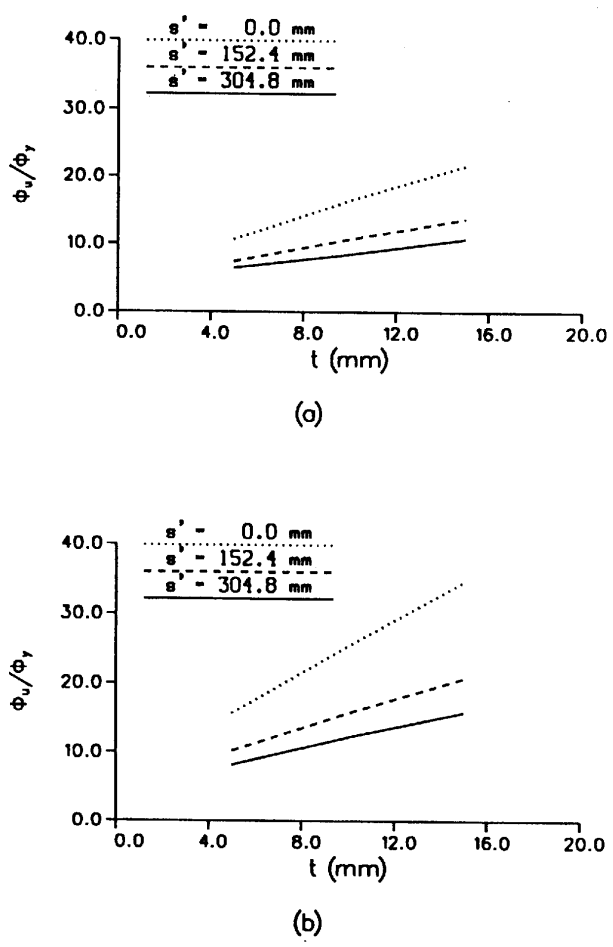

Fig. 10—Ductility versus thickness for circular column [f_{co}' = 20.67 MPa (3000 psi), P/P_o = 0.1]: (a) E-glass; (b) carbon fiber

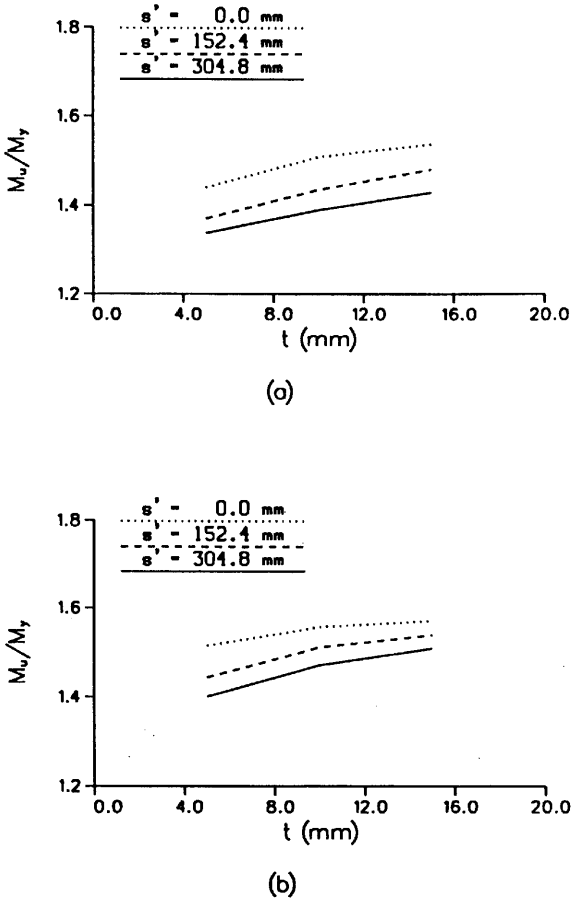

Fig. 11—Moment versus thickness for circular column [f_{co}' = 20.67 MPa (3000 psi), P/P_o = 0.2]: (a) E-glass; (b) carbon fiber

Fig. 11 shows the relationship between the moment ratio M_u/M_y and strap thickness t where M_y is the moment of unconfined column at first yield of tension steel, and M_u is the ultimate moment of confined column. From this graph, it can be seen that, as the thickness of the strap increases, the moment ratio is also increased. The rate of increase in the moment ratio, the slope of the curve, decreases slightly as the strap thickness increases.

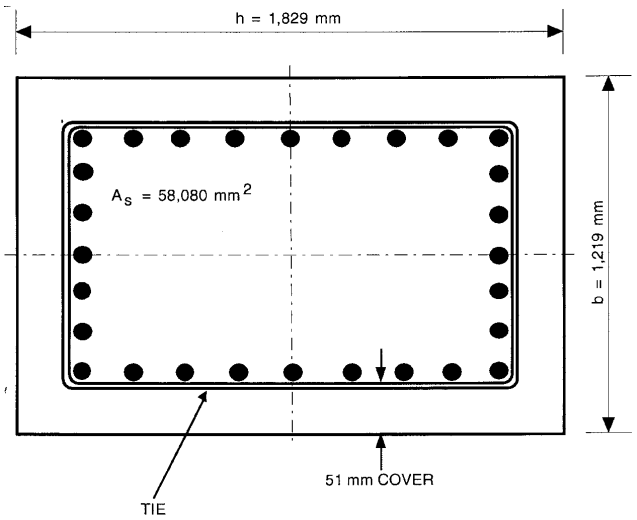

Fig. 12—Cross section and reinforcement details of rectangular column used in parametric study

Rectangular columns

Fig. 12 shows the cross section of the rectangular column used in the parametric study. Grade 60 longitudinal steel reinforcement was used in the analysis of this column. Fig. 13(a) through (c) shows the interaction diagrams and curvature ductility curves for a typical retrofitted column. Fig. 14 shows the relationship between the ductility factor φ_u/φ_y and thickness t. As can be seen from these figures, the same benefits as those discussed for circular columns can be observed for rectangular columns strengthened with high-strength composite straps. The plots of the curvature of ductility versus strap thickness also indicates that the ductility increases as the strap thickness increases, although, however, at a slower rate for wider spacings of the strap, as indicated by the smaller slopes as spacing increases.

To compare the effectiveness of E-glass and carbon fiber straps for retrofitting of concrete columns, the column shown in Fig. 6 was analyzed for a case where the confining force of the strap was kept constant. The strap was 152 mm (6 in.) wide and fully confined the column, that is, the clear spacing between straps was zero. Due to the higher strength

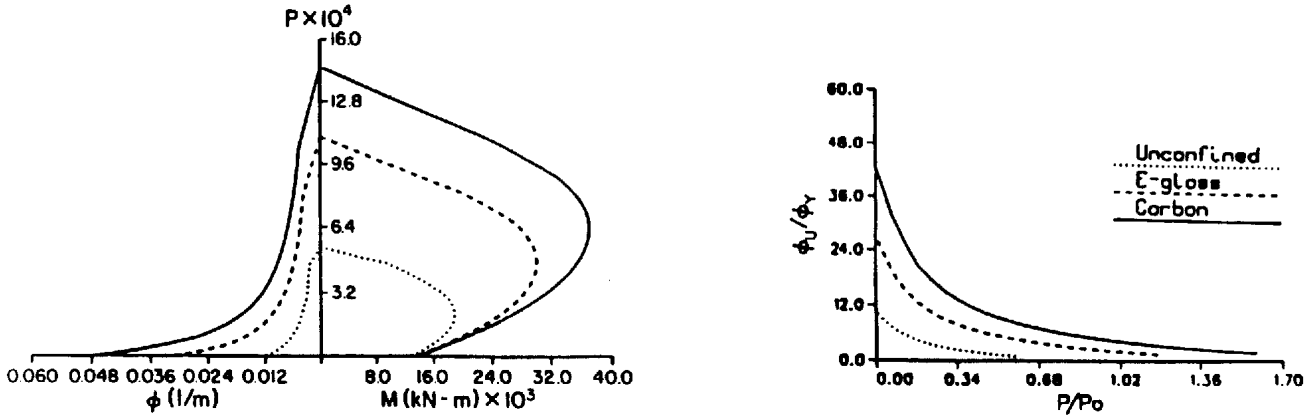

a) Column R3T5S´O

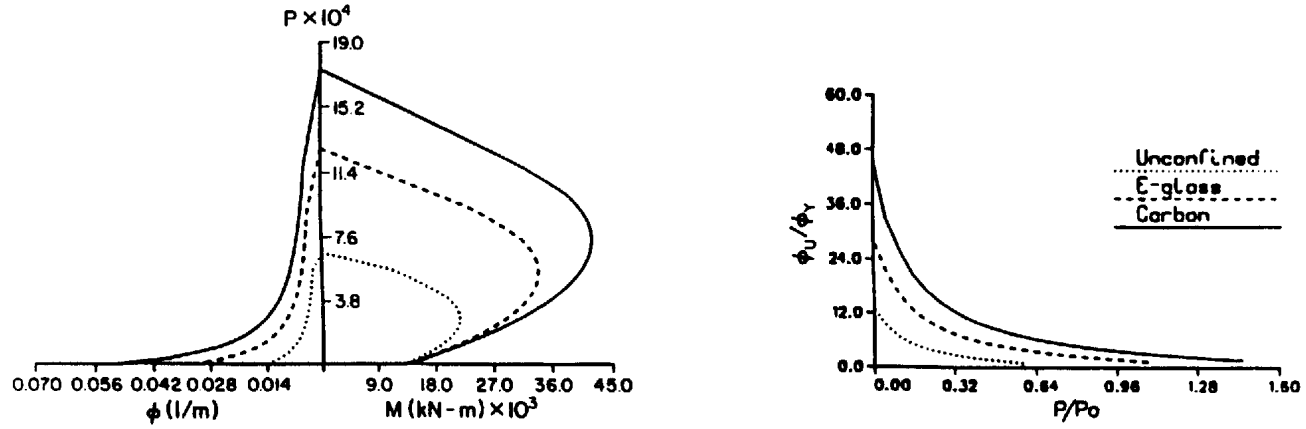

b) Column R4T5S´O

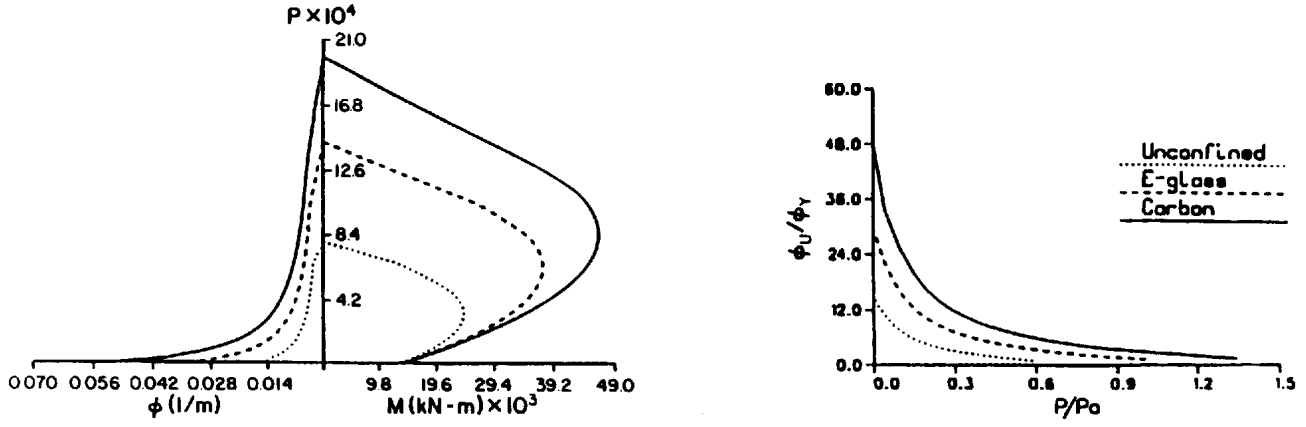

c) Column R5T5S´O

Fig. 13—Interaction diagram and ductility factor of rectangular column for three different concrete compressive strengths

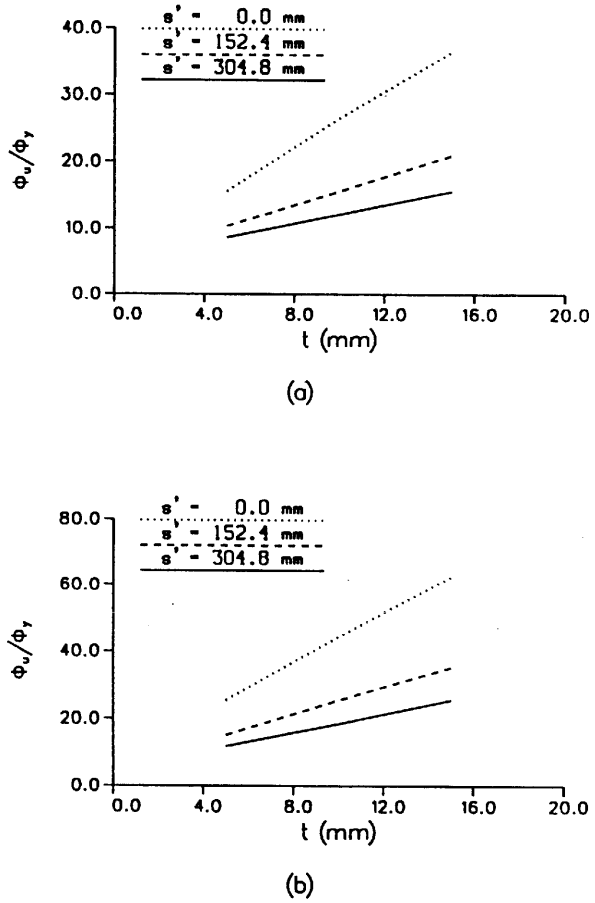

Fig. 14—Ductility versus thickness for rectangular column [f_{co}' = 20.67 MPa (3000 psi), P/P_o = 0.1]: (a) E-glass; (b) carbon fiber

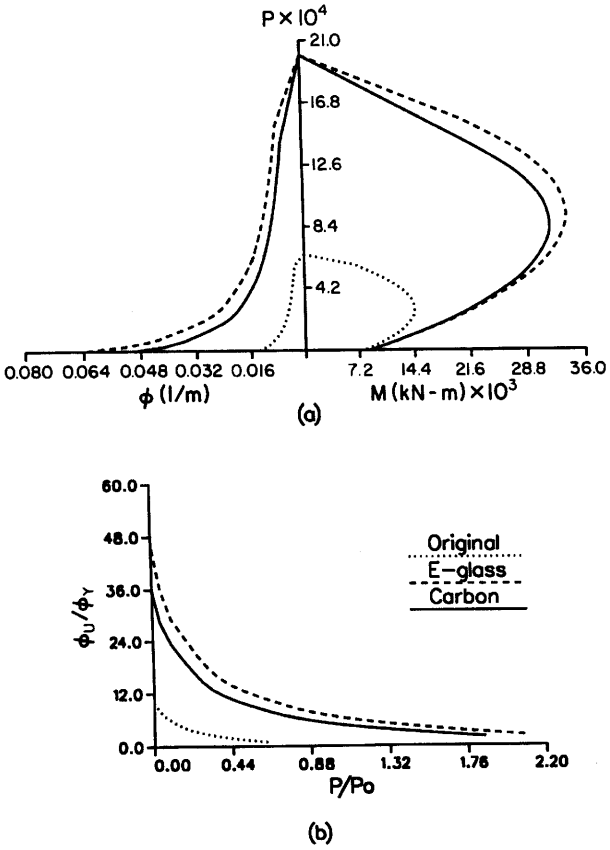

Fig. 15—Interaction diagram and ductility factor of column C5xS′O for E-glass and carbon fiber straps with the same tensile strength

of the carbon fiber strap, and to keep the confining force constant, a larger thickness was used for the E-glass strap. The thickness of the E-glass strap was 25 mm (1 in.), and the thickness of the carbon fiber strap was 10 mm (0.4 in.).

Fig. 15 shows, with the dashed line, the interaction diagram and curvature ductility curve of the column confined with E-glass strap. The solid and dotted lines represent curves belonging to the column confined with the carbon fiber strap and the column prior to strengthening, respectively. Comparing the solid and dashed lines, it can be seen that confinement with E-glass results in a slight increase in both strength and ductility beyond those for confinement with carbon fiber straps. Considering that the cost of carbon fiber is significantly more than that of E-glass, well in excess of the thickness ratio of 2.5, E-glass straps apppear more promising for field application of this technique.

CONCLUSIONS

The analytical studies performed on concrete columns strengthened with composite straps indicate that this strengthening method can be used to increase effectively the strength and ductility of seismically deficient concrete columns. The following conclusions are drawn from the results of the study.

1. The stress-strain models for concrete confined with composite straps indicate significant increases in compressive strength and strain at failure when compared with the stress-strain behavior of unconfined concrete.

2. Although E-glass has a larger elongation at failure than carbon fiber, carbon fiber has a larger energy-absorbing capacity, indicated by its larger area under the stress-strain curve. Based on an energy balance approach, this results in an increase in ultimate axial load and ductility for strengthening with carbon fiber that is larger than that for strengthening with E-glass, if the volumes of straps are equal.

3. The increase in the maximum moment capacity is less than that in the ultimate axial load and ductility factor. This behavior is desirable in seismic strengthening of concrete columns because it results in a ductile flexural failure mode rather than a brittle shear mode of failure.

4. The rate of increase in the ultimate axial load, ductility, and maximum moment capacity decreases for increasing concrete compressive strength.

5. The ductility factor increases linearly with increase in strap thickness; however, the rate of increase in ductility factor decreases as strap spacing increases.

At the present time, a number of circular and rectangular concrete columns are being retrofitted and tested under reversed inelastic cyclic loading at the University of Arizona.

The analytical models described in this paper will be modified to include the effects of cyclic loading, and their results will be compared with measured results from the experiments.

ACKNOWLEDGMENTS

This work was sponsored by the National Science Foundation (Grant No. MSS-9022667 and MSS-9257344). The support of the National Science Foundation is greatly appreciated.

NOTATION

A_{cc} = gross area of concrete

A_{cc} = effective area of concrete enclosed by composite strap

A_e = area of effectively confined concrete core

A_{st} = cross-sectional area of composite strap

b = width of rectangular cross section

d_s = diamter of column

E_c = modulus of elasticity of concrete

E_{sec} = secant modulus of elasticity of confined concrete at peak stress

f_c = compressive strength of concrete

f_l = lateral pressure from transverse reinforcement

f_{sl} = stress in longitudinal steel reinforcing bars

f_{st} = stress in composite strap

f_{us} = ultimate strength of composite strap

f_{cc}' = compressive strength of confined concrete

f_{co}' = compressive strength of unconfined concrete

f_l' = effective lateral confining pressure

h = height of rectangular cross section

k_e = confinement effectiveness coefficient

M_y = moment at first yield of tension steel of unconfined column

M_u = moment at failure of confined column

P = axial load

P_o = ultimate axial load of unconfined column

S = width of composite strap

S' = clear spacing between composite straps

t = thickness of composite strap

U_{cc} = ultimate strain energy per unit volume of confined concrete

U_{co} = unconfined concrete

U_{sl} = energy required to maintain yield in longitudinal steel in compression

U_{st} = ultimate strain energy per unit volume of composite strap

ε_c = longitudinal compressive strain of concrete

ε_{cc} = strain at maximum concrete stress f_{cc}'

ε_{co} = strain at maximum concrete stess f_{co}'

ε_{cu} = ultimate strain of confined concrete

ε_{sl} = strain in longitudinal steel reinforcing bars

ε_{st} = strain in composite strap

ε_{us} = ultimate strain of composite strap

ρ_{cc} = ratio of area of longitudinal reinforcement to gross area of concrete

ρ_s = volumetric ratio of confining strap to concrete core

ϕ_y = curvature at first yield of tension steel

ϕ_u = curvature at failure of confined column

REFERENCES

1. Chai, Y. H.; Priestley, M. J. N.; and Seible, F., "Seismic Retrofit of Circular Reinforced Concrete Bridge Columns," *ACI Structural Journal*, V. 88, No. 5, Sept-Oct. 1991, pp. 565-584.

2. Saadatmanesh, H., and Ehsani, M. R., "Fiber Composite Plates Can Strengthen Beams," *Concrete International: Design & Construction*, V. 12, No. 3, Mar. 1990, pp. 65-71.

3. Saadatmanesh, H., and Ehsani, M. R., "R/C Beams Strengthened with GFRP Plates: Experimental Study," *Journal of Structural Engineering*, ASCE, V. 117, No. 11, Nov. 1991, pp. 3417-3433.

4. An, W.; Saadatmanesh, H.; and Ehsani, M. R., "R/C Beams Strengthened with FRP Plates: Analysis and Parametric Study," *Journal of Structural Engineering*, ASCE, V. 117, No. 11, Nov. 1991, pp. 3434-3455.

5. Katsumata, H.; Kobatake, Y.; and Takeda, T., "Study with Carbon Fiber for Earthquake-Resistant Capacity of Existing Reinforced Concrete Columns," *Proceedings of the Ninth World Conference on Earthquake Engineering*, Aug. 2-9, 1988, Tokyo, V. 7, pp. 517-522.

6. Zamichow, N., "S.D. Research May Butress State's Bridges," *Los Angeles Times*, July 26, 1991, Sec. A:1, p. 22.

7. Hoskin, C. B., and Baker, A. A., "Composite Materials for Aircraft Structures," *AIAA Education Series*, American Institute of Aeronautics and Astronautics, Inc., New York, 1986.

8. Pleiman, L. G., *Tension and Bond Pull-Out Tests of Deformed Fiberglass Rods*, Vega Technologies, Marshal, Arkansas, 1987.

9. *FIBERITE Materials Handbook*, Imperial Chemical Company (ICI), Mar. 1989, p. v.b-16.

10. *FIBERITE Materials Handbook*, Imperial Chemical Company (ICI), Mar. 1989, p.v. b-53.

11. Mander, J. B.; Priestley, M. J. N.; and Park, R., "Theoretical Stress-Strain Model for Confined Conrete," *Journal of Structural Engineering*, ASCE, V. 114, No. 8, Aug. 1988, pp. 1804-1826.

12. Popovics, S., "Numerical Approach to the Complete Stress-Strain Curves for Concrete," *Cement and Concrete Research*, V. 3, No. 5, 1973, pp. 583-599.

13. Mander, J. B.; Priestley, M. J. N.; and Park, R., "Seismic Design of Bridge Piers," *Research Report* No. 84-2, University of Canterbury, New Zealand, 1984.

14. Richart, F. E.; Brandtzaeg, A.; and Brown, R. L., "Study of the Failure of Concrete under Combined Compressive Stresses," *Bulletin* 185, University of Illinois Engineering Experiment Station, Champaign, 1928.

15.Schickert, G., and Winkler, H., "Results of Tests Concerning Strength and Strain of Concrete Subjected to Multiaxial Compressive Stresses," *Deutscher Ausschuss for Stahlbeton* (Berlin), No. 277, 1979.

16. Scott, B. D.; Park, R.; and Priestley, M. J. N., "Stress-Strain Behavior of Concrete Confined by Overlapping Hoops at Low and High Strain Rates," ACI JOURNAL, *Proceedings* V. 79, No. 1, Jan.-Feb. 1982, pp. 13-27.

17. Sheikh, S. A., and Uzumeri, S. M., "Strength and Ductility of Tied Concrete Columns," *Journal of Structural Division*, ASCE, V. 106, No. 5, 1980, pp. 1079-1102.